Single-file diffusion of interacting particles in a finite-sized channel

Jean-Baptiste Delfau, Christophe Coste, Catherine Even, Michel Saint Jean

Single-file diffusion of interacting particles in a finite-sized channel

J. B. Delfau, C. Coste, C. Even, and M. Saint Jean
Laboratoire MSC, UMR CNRS 7057 et Université Paris Diderot-Paris7 Bâtiment Condorcet, 10 rue Alice Domon et Léonie Duquet, 75205 Paris Cedex 13, France

(Received 21 May 2010; revised manuscript received 6 July 2010; published 20 September 2010)

We study the dynamics of charged macroscopic particles (millimetric steel balls) confined in a linear channel of finite length, sufficiently narrow to avoid particles crossing. We show that their individual response to thermal fluctuations strongly depends either on their position in the channel or the local potential they experience. Three different dynamical regimes are identified. At small times, a "free regime" takes place, with the outermost particles exhibiting the highest diffusion coefficient. This effect results from an "echo" of the thermal fluctuations reflected by the channel wall. Then, forbidden crossing induces a correlated regime similar to single file diffusion. Surprisingly, the corresponding mobility increases with the local potential. Lastly, the finite length of the channel induces the saturation of fluctuations. We show that those behaviors may be described heuristically with the help of models for N hard-core interacting particles diffusing in a finite channel of length L, provided that we replace the uniform interparticle distance L/N by a characteristic distance $(k_BT/K)^{1/2}$ built upon the temperature T and the stiffness K of the local potential. It provides a very satisfactory estimate for the fluctuations sizes, whereas they are greatly overestimated assuming hard-core interactions.

DOI: 10.1103/PhysRevE.82.031201 PACS number(s): 51.20.+d, 05.40.−a, 02.50.Ey, 74.25.−q

Single-file diffusion (SFD) describes the diffusion of particles in a channel wherein any crossing is forbidden. During the last few decades, many studies have explored this one-dimensional (1D) diffusion for infinite systems of hard-core interacting particles [1–5]. The studies which investigate the diffusion of long-range interacting particles in a finite length channel [6,7] are less frequent. Nevertheless, this situation corresponds to various interesting physical phenomena, such as the dynamics of vortices in stripe superconductors [8] or of ions in linear electrostatic traps [9]. To get a better understanding of this particular diffusion and determine its main characteristics, we have studied the behavior of a set of metallic balls interacting with tunable electrostatic forces, diffusing in a rectilinear closed channel and submitted to a mechanical shaking simulating a thermal agitation. The dependency of the diffusion upon the particle position is analyzed by considering the local potential experienced by each particle. We show in particular that a "fluctuation echo" is associated to the particles near the channel edges, which is responsible for the increase of particle mobility with the local potential.

Many important results concerning SFD in infinite or circular channels (ensuring periodic boundary conditions) have been previously found both theoretically and experimentally. SFD systems are generally modelized by a set of particles with hard-core interaction undergoing a random walk along an infinite line [1–3]. For these infinite correlated systems, the mean square displacement (hereafter m.s.d.) $\langle x(t)-\langle x\rangle\rangle^2$ (where $\langle\ldots\rangle$ means ensemble averaging over all the trajectories) varies asymptotically as $t^{1/2}$ at large times. Indeed, after an initial free diffusion, the collective motion of particles have to be considered since the displacement of one particle over a long distance in one direction requires the motion of other particles and slows down the diffusion. The continuous evolution from free diffusion toward SFD regime when mutual passages are progressively forbidden has been well discussed [4]. The $t^{1/2}$ scaling at large time is specific to the case of an infinite set of diffusing particles. Indeed, for a finite number of particles, the evolution of m.s.d. remains linear with time with a diffusion constant strongly depending upon the particle place in the sequence [5]. A $t^{1/2}$ scaling is also observed in cyclic 1D systems [2,10–12,17]. In this latter case, a return to an uncorrelated diffusion scaling at very long times happens, the circular set of particles behaving as a single effective particle, with a mass equal to the sum of the masses of all the particles, freely diffusing in the circular channel [2,11].

Most of those theoretical studies are restricted to hard-core interaction but recently, two important results have been obtained for particles correlated by long-range interaction. It was at first shown that a 1D system of particles interacting with an arbitrary repulsive force, in the thermodynamic limit, exhibits the typical SFD $t^{1/2}$ scaling, provided that the correlation length between the particles is of finite range [13,14]. Second, simulations have demonstrated that the m.s.d. of long-range interacting particles in cyclic systems vary as a t^{α} power law with α close to 0.5, slightly varying with the particle interaction intensity and the damping [12,14].

Experimentally, SFD behavior have been observed in extended quasi 1D geometries, as for ion transport in biological membranes [18], molecules channeling in zeolithes [19,20] or in semicrystal of polymers [21], protein diffusion along DNA [22] or nanosized particles transport in nano-fluidic devices [23,24]. However, some results seemed conflicting. For instance, nuclear magnetic resonance studies [4,25] and quasielastic neutron scattering experiments [25,26] using organic molecules in porous materials either concluded to subdiffusive transport [4,25] or to classical diffusion [25,26] with apparently the same experimental conditions. In order to clarify this point, experiments on colloidal particles with magnetic [27] or electric [28,29] dipolar interactions diffusing in a circular channel obtained by photolithography [27,28] or optical tweezer trapping [29] have been performed. While free diffusion is always observed for short times, the long time behavior of the m.s.d. is not that clear, some authors suggesting a $t^{1/2}$ scaling in agreement with the

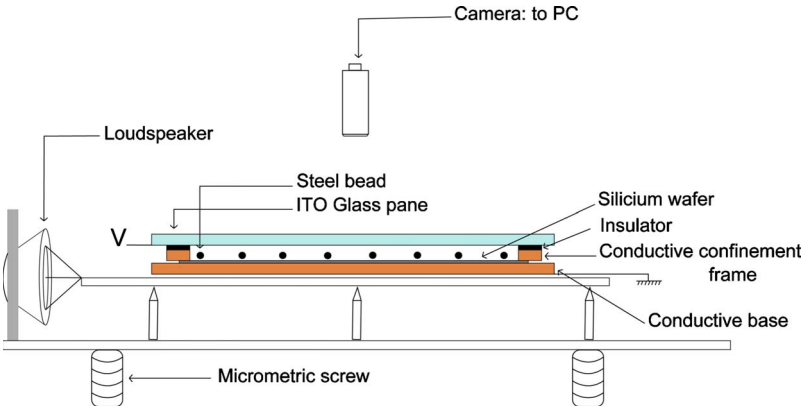

FIG. 1. (Color online) Experimental set up.

theoretical predictions [27,29] whereas others invoke hydrodynamic coupling effects [28]. More recently, we have shown that metallic balls with screened electrostatic interaction diffuse slightly slower than in the case of a hard-core interaction [15–17], the power law coefficient $\alpha < 0.5$ depending upon the interaction magnitude [15]. More surprisingly, this diffusion is enhanced in the case of diffusion in a fluctuating potential [16].

All these results have to be reconsidered in the case of finite channels since the particle diffusion then depends upon the particle position in the channel [6,7]. In Sec. I, we present our experimental setup and methods. The local potential explored by the balls and the main results for the balls diffusion are reported in Sec. II. For all particles, we exhibit three successive dynamical regimes. Their evolution with the interparticles interaction and with effective temperature depends on the local potential experienced by the considered ball. We focus on the "fluctuation echo" that may explained why, in the correlated SFD regime in a finite channel, the particles mobility increases with the local potential. These results will be discussed in Sec. III. The SFD description by a single effective diffusion as for infinite systems cannot be relevant for finite channels since all the particles are distinct with respect to the confinement frame. However, we shall see that the SFD models of diffusion in a finite channel can be adapted in order to introduce this position dependence together with the long-ranged interactions.

I. EXPERIMENTAL SET UP AND METHODS

In our experiment, stainless steel balls of radius $R = 0.4$ mm and weight $m = 2.15$ mg are located in a horizontal plane condenser of height $h = 1.5$ mm. In order to capture the balls positions by a camera placed above the experimental device, the upper electrode is a transparent conductor glass. The bottom electrode is a doped-silicon wafer. Between these two electrodes, a metallic frame is intercalated and confines the balls in a linear channel of width selected to forbid any ball crossing. This frame is in electric contact with the bottom electrode, and insulated with a mylar film from the upper one. In order to charge the balls, a tunable voltage V of about 1 kV is applied between the electrodes (Fig. 1).

In a previous study, we have shown that the interaction potential between two balls is well described through a modified Bessel function of the second kind K_0. It reads

$$U(r) = \varepsilon_0 V^2 h e_0 K_0(r/\lambda), \tag{1}$$

where ε_0 is the vacuum permittivity, $e_0 \approx 0.71$ is a numerical constant and the screening length λ is about 0.3 h $= 0.5$ mm and independent of the applied potential V [30]. This expression has been experimentally validated and shown to give accurately the equilibrium configurations of N balls confined in a ring, with $5 \leq N \leq 30$ [30].

To introduce a thermal noise, the whole cell is fixed on loudspeakers supplied by a white noise voltage. It has been previously shown that the shaking amplitude stands for an effective temperature [17,31]. This temperature is determined *in situ* by measuring the m.s.d. of a single ball confined by an independent circular frame located on the same cell [31]. We thus have a well controlled experimental system which allows to follow the individual trajectories of interacting particles over a long period of time.

The shape of the confinement potential depends upon the applied potential V and the channel dimensions. Let l be its width and L its length, with $l < L$. The beads have to be aligned along a straight line in their equilibrium configuration. It could be tempting to apply a large potential between the electrodes but in this case the electrostatic pressure at the chain extremities could favor an unwanted zigzag configuration. The channel size has also to be well chosen. For a too wide channel, the transverse confinement potential is too flat along the channel axis, and a transition toward the zigzag configuration happens. For a too narrow channel, even if the 1D configuration seems geometrically favorable, the superposition of the two repulsive contributions of the long walls induces a too small transverse confinement, once again favoring a zigzag configuration. So a compromise has been found: the applied potential V varies between 1000 and 1400 V while the channel width l and length L are 4 and 60 mm, respectively.

Moreover, for a given channel, the relative importance of the electrostatic pressure at the ends of the chain with respect to the interparticle repulsion also depends upon the number of particles. The results presented here have been obtained with a system of $N = 32$ balls for which the roles of the interparticle and confinement contributions in the diffusion can be clearly distinguished. The outermost balls feel a strong

FIG. 2. Line of balls in the channel.

longitudinal repulsive field due to the channel edge whereas this contribution is negligible for the particles located in the central part.

For each applied voltage and effective temperature, the positions of the particles are captured by a video recording of 30 000 images, with a typical time between two snapshots of 10 ms, which is much smaller than the relaxation time associated to the shaking process and determined from the fluctuation-dissipation relation [15,32]. We thus get for the ith particle a recorded trajectory $\{(x_i(t), y_i(t)\}$ where $x_i(t)$ [respectively, $y_i(t)$] is the instantaneous coordinate along (respectively, normal to) the channel axis with the origin at the left edge (respectively, on the axis).

For each particle, the diffusion is characterized by its position distribution and the evolution with time of its mean square displacement. To improve the statistics, we built a set of statistically independent effective trajectories indexed by t': $\{x_i(t,t') = x_i(t+t') - x_i(t')\}$. The corresponding m.s.d. $\sigma_i(t)$ is then defined by

$$\sigma_i(t) = \langle\langle [x_i(t,t') - \langle x_i(t,t')\rangle]^2\rangle\rangle \quad (2)$$

where the first brackets $\langle \ldots \rangle$ refer to the usual average over each effective trajectory $\{x_i(t,t')\}$ while the second one is over all initial times t'.

II. EXPERIMENTAL RESULTS

A. Nonuniform distribution of equilibrium positions and local potentials.

The ball positions in the channel are shown on Fig. 2. Since the interball repulsion is strong enough to locate the outer ball near the edge, the channel is quasicompletely occupied. However, this distribution is not uniform, the interball distance d_i [defined as the distance between the ith and $(i+1)$th balls] increasing roughly quadratically with the particle distance from the channel center as shown in Fig. 3. It is noteworthy that in comparison to the uniform interball distance L/N, the outermost ball is farther from its neighbor whereas the other balls are closer. This nonuniform distribution is characteristic of interacting particles confined in a finite-sized channel, resulting from the competition between the interball force which favors the chain expansion and the repulsion by the edge which encourages its compression.

If we consider the particle position histograms, they are symmetric for the inner balls, but a progressive asymmetry takes place as the balls depart from the channel center, the most asymmetric histograms being associated to the outermost particles (Fig. 4). However, such histograms are markedly different from those obtained for of hard-core interacting particles [6,7]. In this case the outermost ball histograms are not bell-shaped, and have much greater amplitude than the others. For hard-core interactions, the outermost ball can hit the wall which acts like a mirror, the resulting position distribution being the superposition of the incident and reflected ball distributions [33]. In our case, by contrast, this superposition is less effective since the repulsive confinement is a long-range interaction and then the balls never hit the channel edge. This is the first difference between the hard-core interaction case and the long-range one.

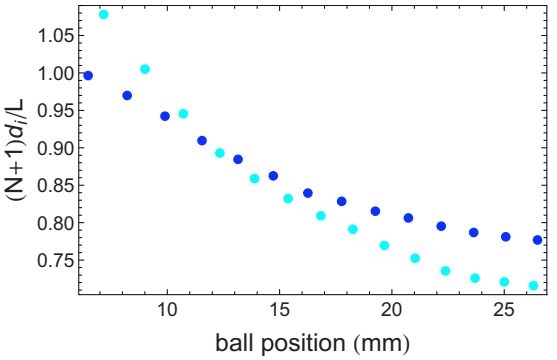

FIG. 3. (Color online) Plot of the dimensionless interball distance d_i, normalized by $L/(N+1)$, as a function of the ball position in the chain (in mm) for $V=1000$ V (light blue—light gray) and $V=1300$ V (dark blue—dark gray). The left edge and the center of the channel are located at $x=0$ and $x=30$ mm, respectively.

The local potential experienced by each ball can be determined from its equilibrium position. Knowing the analytical expression of the interparticle interaction, Eq. (1), and the equilibrium positions of every ball, we may calculate the interball force f_i exerted on each ball i in the channel. This force obviously decreases with the applied voltage. It decreases as the ball approaches the channel edge [Fig. 5(a)] because the distances between adjacent balls increase. The confinement forces are then extracted from those interball forces by considering that each ball is in equilibrium under the action of the confinement force, and the forces from its neighbors. The obtained confinement repulsive force is presented in Fig. 5(b). We can notice that near the channel edge, the confinement potential is strong, rapidly increasing with the applied voltage. Inside the channel, it is very small, slightly decreasing as the particle gets closer to the channel center and is roughly independent of the applied potential.

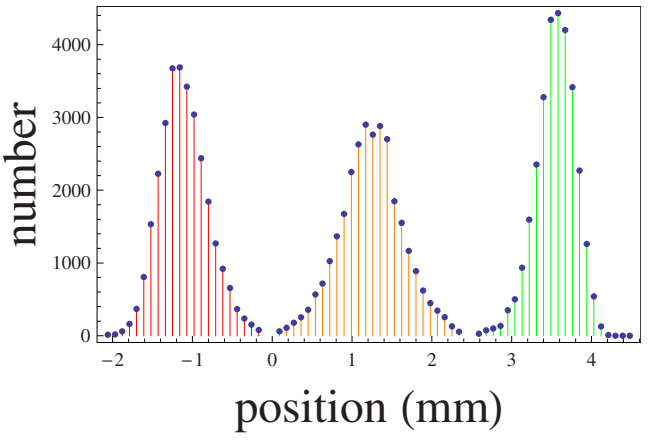

FIG. 4. (Color online) Position histograms of the first, 16th, and 32th balls, from left to right, for $V=1300$ V and $T=10^{12}$ K. For convenience, the histograms have been translated.

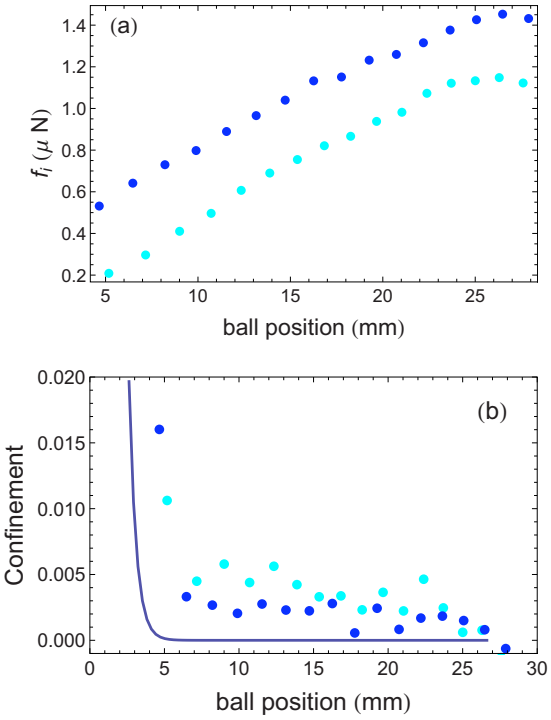

FIG. 5. (Color online) (a) Plot of the interball interaction (in μN) as a function of the ball positions in the channel (in mm). (b) Plot of the dimensionless confinement force (in unit of $\varepsilon_0 V^2$) as a function of the ball positions in the channel (in mm) for $V=1000$ V (light blue—light gray-dots) and 1300 V (dark blue—dark gray-dots). Notice that the outermost balls experience abrupt variations of the confinement potential. The solid line is the 2D estimate detailed in the appendix.

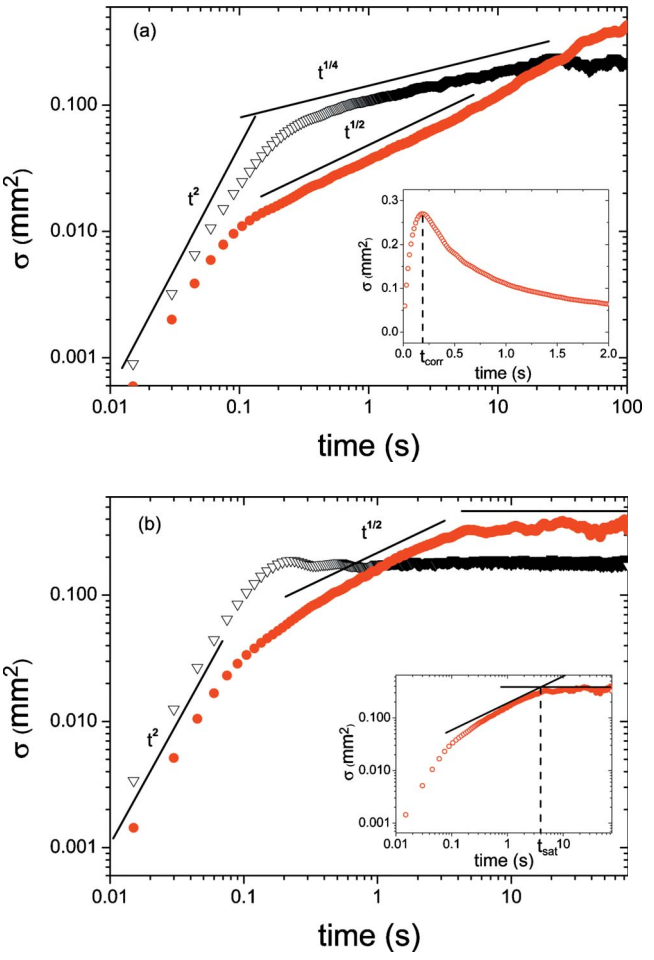

FIG. 6. (Color online) Plot of the m.s.d. (in mm^2) of the central (filled disks) and the outermost balls (empty triangles) as a function of time (in s.) for $V=1000$ V (a) and 1300V (b). Three different regimes can be observed. Their extensions vary according to the ball position and the applied voltage. Notice the "curve crossing" which is characteristic of the diffusion in finite channel and indicates different dynamic regimes according to the ball position. The insert in 6a and 6b, respectively, explain the measurements of t_{corr} and t_{sat}.

The rigorous calculation of this confinement force requires the (numerical) resolution of the Laplace equation with Dirichlet boundary conditions on the confining frame and on the balls to get the electrostatic potential and the electric field. Then the surface charge distribution on a ball must be determined in order to calculate the integrated confinement force. However, to understand the main relevant features of the measured confinement force, it is sufficient to estimate it with a simple model of a point charge in the two-dimensional (2D) potential in the channel edge geometry. This is done in the Appendix, and the result is the solid line plotted in Fig. 5(b), which exhibits a reasonable agreement with the experimental data. We observe again that the outermost balls actually feel the confining potential of the channel edges.

So we can consider the inner balls as moving in a local potential which is the superposition of strong repulsive potentials due to their two neighbors and a very small confinement contribution whereas the outermost balls experience by contrast a strong and abrupt repulsive confining potential and a slightly varying repulsion due to their relatively far neighboring balls.

B. Diffusive behaviors

The time evolution of the m. s.d. of a confined ball looks like a gradual slowing down, however three different regimes of diffusion can be identified. After an initial free diffusing regime ($t<t_{corr}$), the balls undergo a correlated diffusion ($t_{corr}<t<t_{sat}$) during which their m.s.d. scales as $t^{1/2}$ until finally, since the channel size is finite, their m.s.d. reaches saturation values ($t_{sat}<t$) less than a few per cent of the interball distance (Fig. 6). The time t_{corr} is somewhat arbitrarily defined as the time associated to the maximum of $\sigma_i(t)/t$ since the m.s.d. varies as t^α with $\alpha \geq 1$ before t_{corr} and $\alpha<1$ for a correlated diffusion [see the insert Fig. 6(a)]. We define t_{sat} by the crossing of the two straight lines corresponding to the asymptotic behaviors of the correlated and saturation regimes in log-log scales, as shown in the insert of Fig. 6(b) (If we apply the previous method, defining t_{sat} as the maximum of $\sigma_i(t)/t^{1/2}$ we get too scattered data). Those three diffusion regimes are observed for each ball, whatever the voltage or temperature that is applied. Whatever the m.s.d. amplitude, its saturation value at asymptotically large time as well as the two crossover times t_{corr} and t_{sat} depend

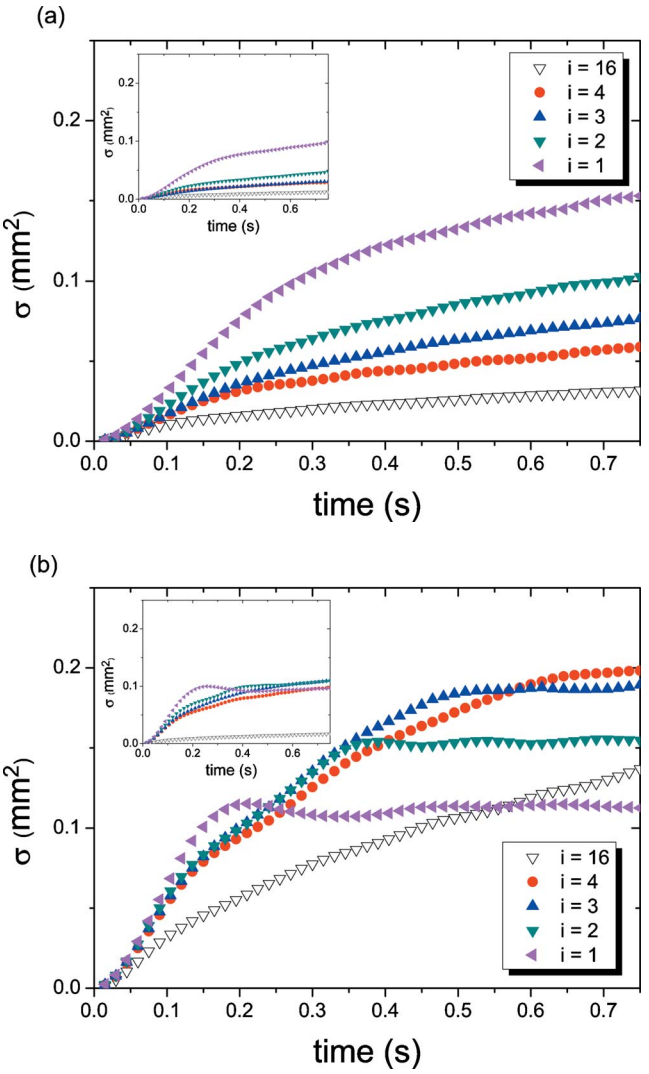

FIG. 7. (Color online) Plot of the m.s.d. (in mm^2) of the first four balls closest to the channel edge and of the central ball, as a function of time (in s.), for $V=1000$ V (a) and 1300 V (b), $T=10^{12}$ K. Only short times evolution is displayed. The highest diffusion coefficient is always associated to the outermost ball and the diffusion slows down as the particle gets closer to the channel center. The diffusion increases with the applied voltage suggesting the particular role played by the confinement. Notice also the evolution of the crossover times with the ball positions. In insert, the corresponding curves for $T=8\ 10^{11}$ K.

on the ball position, the applied voltage and less significantly on the effective temperature. For instance, the duration of the correlated diffusion regime is much longer for the inner balls than for the outermost balls when the applied voltage is high [Figs. 6(a) and 6(b)].

More precisely, for short times ($t<t_{corr}$), each ball moves independently without efficiently interacting with its neighbors and therefore performs a free particle diffusion (Fig. 7). Two time dependencies can be observed in this regime according to the applied voltage or the ball positions. When the local potential explored by the considered ball is flat because it is far from the other balls and the applied voltage is small, the classical linear diffusion regime of a free particle can be

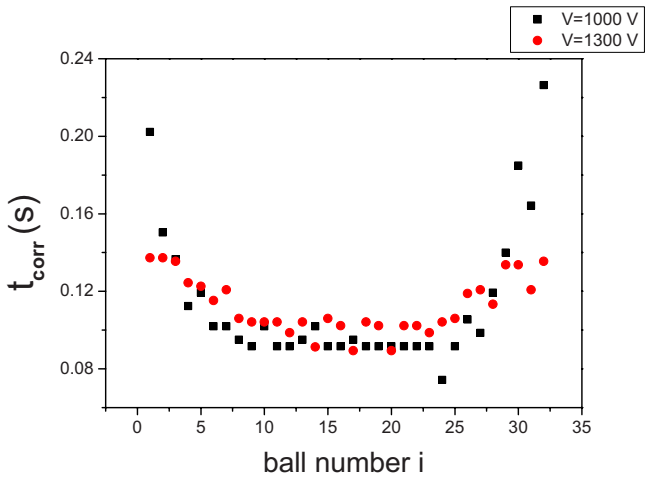

FIG. 8. (Color online) Evolution of the crossover time t_{corr} (in s.) according to the ball position for $V=1000$ and 1300 V.

observed after an initial quadratic regime. On another hand, if the considered ball is charged by a strong enough voltage and is located very close to its neighbors or near the channel edge, it moves as a free particle in a local potential looking like the bottom of a parabolic potential, so its m.s.d. varies as t^2.

In these "free diffusion regimes," the diffusion increases with the applied voltage whichever ball we consider. Moreover, for a given applied voltage, the diffusion coefficient increases with the distance of the considered ball from the channel center, the highest coefficients being always associated to the outermost balls (Fig. 7). The duration of this free regime varies also according to the position of the particles and to the applied voltage. For instance, the crossover time t_{corr} increases when the ball gets closer to the channel edge. This time increases also with the applied voltage with a noticeable exception for the outer balls (Fig. 8). We point that the resulting "crossing" of curves observed in Fig. 8 is identical to those observed for the normalized interball distances (Fig. 3) and emphasizes the important role of the confinement potential near the channel edge. We will see this again in the next section. Similar behaviors are observed for all effective temperatures, even if they are less marked as the temperature decreases (Fig. 7, inset).

In the saturation regime ($t>t_{sat}$), the m.s.d. reaches a constant asymptotic value which decreases with the applied voltage, with the distance from the channel center, and increases with the effective temperature (Fig. 9). Moreover, the high values of t_{sat} observed for the inner balls underline the collective nature of the correlation effects. Those balls experience the stronger interparticle force and the smallest interparticle distances, which would result in the most rapid saturation only if they experience a static local potential. On the contrary, because of the correlated motion of their neighbors they reach their saturation last.

During the intermediate times ($t_{corr}<t<t_{sat}$), the m.s.d. roughly varies as $t^{\alpha}(\alpha<1)$ as for a correlated diffusion. For the inner balls which roughly behave like balls embedded in a large system, α is found slightly smaller than 1/2 in agreement with our previous observations in a circular channel

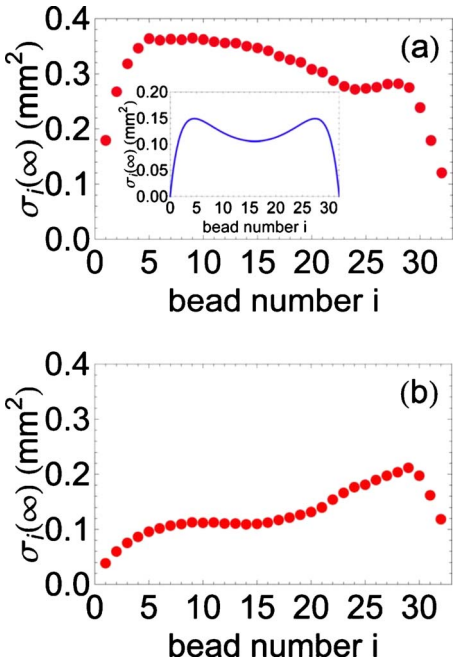

FIG. 9. (Color online) Evolution of the m.s.d. saturation values $\sigma_i(\infty)$, in mm^2, with the ball position for $V=1000$ V (a) and 1300V (b), $T=10^{12}$ K. Insert: The camel back evolution of $\sigma_i(\infty)$ (in mm^2) is obtained if we consider the actual dependence of d_i with the ball number in the expression (2). The order of magnitude is also satisfactorily recovered.

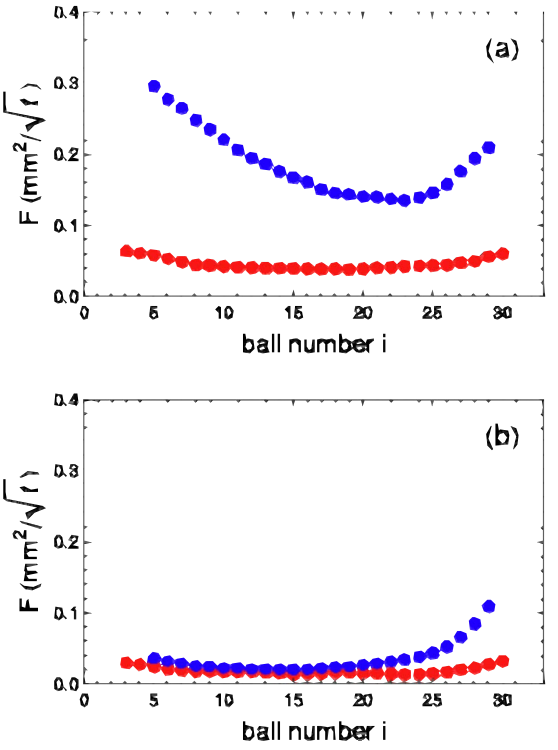

FIG. 10. (Color online) Evolution of the mobility F with the ball position for $V=1000$ (blue—light gray-) et 1300V (red—dark gray-), (a) $T=10^{12}$ K, (b) $T=8\ 10^{11}$ K).

[15,16] and simulations of that same system [12]. For the outermost balls, α is on the contrary slightly higher than 1/2 (Fig. 6). Apart from those small differences, the main point which distinguishes the ball behaviors is the amplitude of the single file mobility F_i, defined as $\sigma_i(t)=F_i t^{\alpha}$ For a given applied voltage, in contrast with the saturated m.s.d. values, the mobilities increase from the central ball to the outer ones as shown in Fig. 10. Moreover, the measured mobilities increase with the applied voltage in spite of the intensification of the repulsive forces. It is noteworthy that this result is in contradiction with either the observations [17] or the theoretical predictions [13] in a circular or an infinite channel. This effect is thus a particularity of confined systems.

The estimations of t_{corr} and t_{sat} show that the longest duration of this correlated regime is obtained for the inner balls charged by a small applied voltage. We can also notice that the saturation times t_{sat} are one to three orders of magnitude larger than the correlation time t_{corr}, whereas simulations for hard-core interaction suggests five orders of magnitude between these two times [6]. This confirms the important role of the long-range interaction which drastically reduces the extension of intermediate correlated regime by limiting the accessible positions of balls.

III. DISCUSSION

No complete theory is devoted to the SFD of long-range interacting particles in a finite channel. Therefore, in order to discuss qualitatively our experimental results, we have adapted the description dedicated to a finite system with hard-core interaction, using an important result concerning the SFD of long-range interacting particles in an infinite system. Since all the experimental results suggest the importance of the local potential on the diffusion behaviors, the basis of our approach is to consider the movements of the ball as a diffusion in a quadratic potential described by a stiffness K. This assumption is suggested, e.g., by the oscillations observed on the m.s.d. of the outermost balls just before saturation, which look like those observed in the transverse diffusion of balls in a circular channel [16] [Fig. 6(b)]. Consequently, we introduce a characteristic length $(k_B T/K)^{1/2}$ (where T is the effective temperature, k_B the Boltzmann constant and K the effective stiffness of the local potential) instead of the uniform distance L/N that is relevant for hard core interactions.

We shall begin with the saturation regime. The exact expression of the saturation values $\sigma_i(\infty)$ obtained for hard-core interacting particles confined in a finite chain with rigid edges is given in references [2,8]. Taking back the expression of Beijeren *et al.* [2] and considering that our experiment corresponds to a very small average occupation of sites and a number of balls $N \gg 1$, the m.s.d. $\sigma_i(\infty)$ could be written,

$$\sigma_i(\infty) = \langle x_i^2 \rangle - \langle x_i \rangle^2 \approx \left(\frac{L}{N}\right)^2 \frac{i(N+1-i)}{N}. \qquad (3)$$

Thus, for hard-core interacting point particles, the m.s.d. of the central ball $i=(N+1)/2$ is $L^2/4N$ whereas that of the outermost one ($i=1$ or N) is $(L/N)^2$. These results are in agreement with the analytical results obtained recently by

TABLE I. Comparison between the m.s.d. at saturation $\sigma_i(\infty)$ measured in our experiments (second and fourth column from left), the estimation provided by Eq. (7) (first and third column) and the simulations of Lizana and Ambjörnsson (Ref. [6] and Eq. (3)) for hard core interactions (last column to the right).

	Calculated $V=1000$ V (mm^2)	Measured $V=1000$ V (mm^2)	Calculated $V=1300$ V (mm^2)	Measured $V=1300$ V (mm^2)	Hard core interaction (mm^2)
Central ball	0.12	0.4	0.11	0.35	27
Outermost ball	0.09	0.25	0.04	0.11	3.3

Lizana *et al.* [6,7] for the particle placed in the middle of the channel and the exact derivation of the variance for the balls at each extremities. A simple rescaling of this expression enables the consideration of the case of particles with finite size Δ,

$$\sigma_i(\infty) = \langle x_i^2 \rangle - \langle x_i \rangle^2 = \left(\frac{L - N\Delta}{N} \right)^2 \frac{i(N+1-i)}{N}. \tag{4}$$

This expression can be adapted to the case of long-range interacting particles by considering that the particles explore at most only a small part of the interparticle distance given by $2(\frac{k_BT}{K})^{1/2}$. We can thus consider that the unexplored region has an effective finite size Δ_{eff} defined by

$$\Delta_{eff} = \frac{L}{N} - 2\left(\frac{k_BT}{K} \right)^{1/2}. \tag{5}$$

Substituting this expression in expression (1), we obtain

$$\sigma_i(\infty) \approx 4\left(\frac{k_BT}{K} \right) \frac{i(N+1-i)}{N}. \tag{6}$$

For the interball distances commonly found in our experiments, we may approximate the K_0 interaction by a logarithmic dependence [30], the effective stiffness K of the interball interaction being then proportional to V^2/d^2 [see Eq. (1)], so that

$$\sigma_i(\infty) \approx 4\left(\frac{k_BT}{K} \right) \frac{i(N+1-i)}{N} \propto \left(\frac{k_BTd_i^2}{V^2} \right) \frac{i(N+1-i)}{N}. \tag{7}$$

According to this expression, $\sigma_i(\infty)$ increases with the temperature, decreases with the applied voltage, and the smallest saturation values are associated to the outermost balls in agreement with the experiments (Fig. 9).

This qualitative explanation gives the same order of magnitude for the calculated and measured saturation values, much smaller than the saturation value $\sigma_i(\infty)$ given by the expression (3) associated to hard-core interaction. For instance, Table I compares the measured m.s.d. to those estimated with expression (7) for the central and the outermost balls from their actual positions in the channel.

We shall now consider the "free regime" at very small times ($t < t_{\mathrm{corr}}$). In the case of hard-core interaction, the time t_{corr} is estimated by $\frac{(L/N)^2}{D}$ where D is the free diffusion coefficient. In the case of long-range interacting particles in an infinite or a cyclic system, it is suggested [13] to replace D by an effective diffusion coefficient D_{eff} given by

$$D_{eff} = \frac{K}{(L/N)^2 k_BT} D. \tag{8}$$

This relation confirms that $(k_BT/K)^{1/2}$ is the relevant distance in the case of interacting particles since the time $t_{\mathrm{corr}} = \frac{(L/N)^2}{D_{eff}}$ is nothing else but the time $t_{\mathrm{corr}} = \frac{(kT/K)}{D}$ of free diffusion on the characteristic distance $(k_BT/K)^{1/2}$. Introducing the interball distance to estimate the potential stiffness, we obtain

$$t_{\mathrm{corr}} = \frac{(kT/K)}{D} \propto \frac{(kTd^2/V^2)}{D}. \tag{9}$$

This description with an effective diffusion coefficient is relevant for a weak local potential only. In the case of strong local potential for which no linear regime has been observed (in the inner and outermost balls cases for instance), it is better to describe the ball movement as a ballistic motion in a roughly parabolic potential. In this case t_{corr} is proportional to the oscillation period,

$$t_{\mathrm{corr}} \propto \frac{1}{K^{1/2}} \propto \frac{d}{V}. \tag{10}$$

Whatever description we consider, t_{corr} increases with the interball distance d and decreases with the applied voltage V, in qualitative agreement with our results. However, this picture is too simple to quantitatively describe this crossover time. Indeed, the calculated t_{corr} are larger than the measured ones. This suggests that when the correlations are strong enough, each particle cannot fully explore its environment before being correlated with other balls.

More surprisingly, it was observed that in this regime, the free diffusion is faster for high applied voltage, the effect being particularly strong for the outermost ball. In our analysis, this effect is specific to finite size systems of long-range interacting particles. Indeed, any position fluctuation of a ball induces a displacement of its neighbors which propagates along the channel and is reflected at the edges. Thus, each ball is submitted to the fluctuations resulting from the thermal bath and from these "echo fluctuations." Its resulting actual effective temperature is then higher than in an infinite system for which such "echo mechanism" is obviously missing. The importance of this effect depends upon the place of the particle in the channel since the fluctuations are damped over a characteristic length. Only the balls not too far from the edges are concerned. It also depends on the interparticle and confinement potential. The higher the repulsive interaction and the closer the edge, the smaller the "echo time."

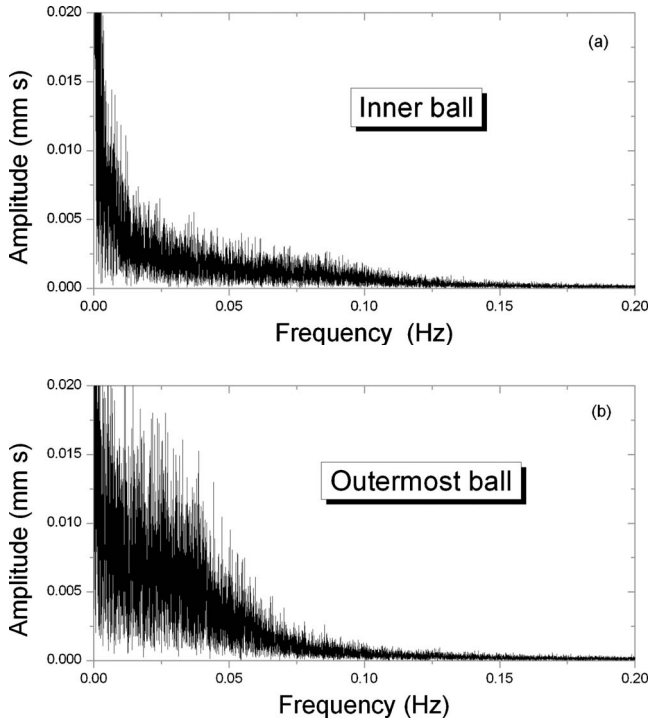

FIG. 11. Spectral analysis of the central (a) and the outermost ball (b) trajectories.

This is observed in our experiment: the free diffusion of the outermost ball is significantly more rapid than those of the inner ones (Fig. 7). A simple picture of this effect in the frame of a Brownian motion can be given by considering the number of steps occurring during the time t. Without echo, the free diffusion coefficient would be given by l^2/τ_c where l is the mean free path and τ_c the collision time. We shall now consider the ith ball, the echo time $t_{\text{echo}}(i)$ associated to this ball is roughly given by $2l_i/v$ where l_i is the distance between the frame edge and the ith ball and v the sound velocity in the system. The velocity v is proportional to V through the square root of the system stiffness [since the interballs potential is proportional to V^2, see Eq. (1)], so $t_{\text{echo}}(i)$ varies as

$$t_{\text{echo}}(i) = 2\frac{l_i}{v} \propto \frac{l_i}{V}. \tag{11}$$

So the step number during the time t is simply given by $t/\tau_c + t/t_{\text{echo}}$. When the ball is far from the edge, $t_{\text{echo}} \gg \tau_c$ and the contribution to the Brownian motion of the "echo mechanism" can be neglected (this effect is even stronger if we also introduce some damping during fluctuation propagation). By contrast, for a ball close to the edge, in particular for the closest ones, t_{echo} and τ_c can be of the same order, so that the number of jumps is higher than for a ball located in the central part of the channel, and the diffusion is then quicker. This assumption is confirmed by the spectral analysis of the fluctuations of ball trajectories which shows that the largest spectral band is obtained for the outermost balls [Figs. 11(a) and 11(b)]. As a consequence, the diffusion coefficient for the balls not too far from the edge varies as V/l_i in qualitative agreement with the observed behaviors discussed in Sec. II B. More quantitatively, we shall indicate that this kind of effect has been previously described in the case of a chain of coupled harmonic oscillators submitted to a fluctuating force and fixed by an extremity on a wall [34].

Lastly, we shall discuss the results obtained in the correlated regime. The inner balls can be understood as embedded in an infinite chain. So in agreement with our previous results on large cyclic systems, they diffuse as t^α with α slightly smaller than 1/2. In contrast, the outermost balls move in a potential created by a fixed edge and a fluctuating ball. Its motion is thus less correlated with those of the other balls than the motion of an inner ball surrounded by other diffusing particles. The behavior of the m.s.d. of an outermost ball, scaling as t^α with α higher than 1/2 may be understood as a compromise between the linear behavior observed when a particle diffuses near a fixed wall [5] and the "correlated diffusion" varying as $t^{1/2}$. Along the channel, the m.s.d. behaviors continuously evolve between these two extremes.

In the frame of the Kollmann theory [13], the mobility F is given by

$$F \propto \left[\frac{Dk_BT}{V^2}\right]^{1/2} \tag{12}$$

and cannot depend on the location of the ball in the channel since this model is devoted to infinite systems only. In order to account for the channel finite size, we insert as for the free regime a diffusion coefficient that includes the "echo effect." The main dependence of the mobility would then be given by

$$F_i \propto \frac{d_i}{V}[k_BT]^{1/2}\left[\frac{V}{l_i}\right]^{1/2}. \tag{13}$$

This expression suggests a correct picture for the evolution according to the ball location but unfortunately cannot explain, even qualitatively, the observed increase of the mobility with the applied voltage. A complete modelization that more precisely includes the echo mechanism, seems to be required.

IV. CONCLUSION

Experiments have been performed to gain a better understanding of the diffusion of a set of particles with long-range interaction, placed in a finite length channel, so narrow that the particles cannot cross each other. We show that the response of a given particle to thermal fluctuations strongly depends on its position and on the local potential it experiences. Following the particle trajectory when time goes on from a given origin, we can clearly identify three different regimes.

At small times, a "free regime" takes place, with the outermost particles exhibiting the highest diffusion coefficient. This effect results from an "echo" of the thermal fluctuations reflected by the channel wall. This behavior is specific of the long-range interaction since it is driven by the elastic propagation of the thermal fluctuation along the chain. Because of

the organization of the particles in a sequence, a correlated regime takes place at longer times, until finally the finite length of the channel induces the saturation of fluctuations. We show that these behaviors may be described at least heuristically, replacing the uniform inter particle distance L/N in the models describing the diffusion of hard-core interacting particles in a finite-sized channel by the characteristic distance $(k_BT/K)^{1/2}$ built upon the temperature T and the stiffness K of the local potential. This lengthscale provides a very satisfactory estimate of the fluctuations sizes, whereas assuming hardcore interactions induces a clear discrepancy with our observations.

The results concerning SFD of confined particles show the specific role of the confinement potential near the channel edges. They could be considered in order to analyze the motion of particles in various strips or pores since in many cases the extremities of such systems induce specific potential barriers. For instance, we could use this kind of effect to discuss the flux-flow noise measured on superconductor strips which largely depends on the vortice motion fluctuations near the sample edge [35].

ACKNOWLEDGMENTS

The authors wish to thank F. Van Wijland for the very helpful discussions concerning the diffusion processes, and B. Mauroy for the 3D calculations of the electric potential.

APPENDIX

In this appendix, we estimate the confinement force exerted on a ball near the channel edge. The cell is modelized as two-dimensional (see Fig. 12), the upper electrode being a straight line at potential V_0 and the lower one, at potential 0, as three straight line segments with two right angles. The largest distance between the two electrodes is h, the smallest one is $a=\varepsilon h$ with $\varepsilon=1/15$. The electric potential in this 2D condenser is given by the complex representation [36]

$$\frac{z}{h} = -\frac{1}{\pi}\left\{\operatorname{arccosh}\left[\frac{(2\zeta+1)\varepsilon^2-1}{1-\varepsilon^2}\right] - \varepsilon \operatorname{arccosh}\left[\frac{(1+\varepsilon^2)\zeta-2}{(1-\varepsilon^2)\zeta}\right]\right\} + i, \tag{A1}$$

where the complex function $\zeta=\exp[i\pi w/V_0]$ depends on the complex potential $w=V-iF$ where V is the electric potential and F the 2D electric flux. The relevant equipotentials are shown in Fig. 12. From a numerical resolution of the three-dimensional (3D) Laplace equation, we have checked that the 3D equipotentials, along the channel axis, are very close to their 2D counterpart.

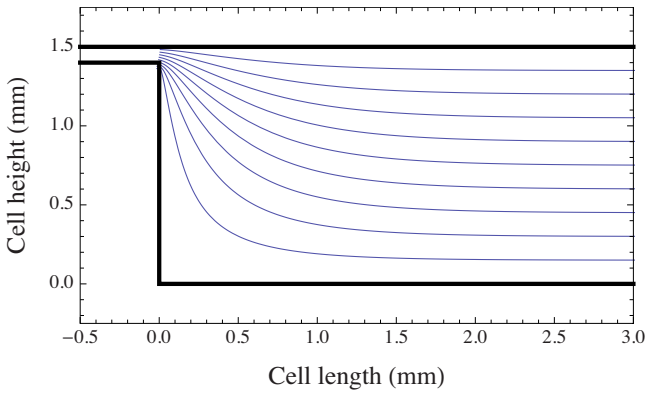

FIG. 12. (Color online) Sketch of the confinement cell showing some equipotentials. The upper thick line is an electrode at potential V_0, the lower thick line the electrode at potential 0. The equipotentials are plotted for $V=iV_0/10$, $1<i<9$. The ratio between the small and large gap between the electrodes is $\varepsilon=1/15$. The vertical axis is along the cell height, and the horizontal axis along its length. All distances are in mm.

We may deduce the electrostatic field from this implicit expression of the potential using the formula

$$E_x - iE_y = -\frac{dw}{dz} = -\left(\frac{d\zeta}{dw}\right)^{-1}\left(\frac{dz}{d\zeta}\right)^{-1}. \tag{A2}$$

The force exerted by this field on a ball in the channel is then estimated by a rather crude approximation. Using the capacity of a conducting sphere, we estimate the electric charge Q of a ball of radius R at $Q\approx 4\pi\varepsilon_0 RV_0$. The force exerted by the channel wall on the ball, along the channel axis, is then QE_x, and we assume that it is applied on the ball center. From Eq. (A1) we deduce the values (V_j,F_j) associated with some points $(x_j,y_j=R)$, and from Eq. (A2) the corresponding values of the electric force $QE_x(x_j,R)$. The result of these calculations is plotted in Fig. 5(b).

[1] T. E. Harris, J. Appl. Probab. **2**, 323 (1965).
[2] H. van Beijeren, K. W. Kehr, and R. Kutner, Phys. Rev. B **28**, 5711 (1983).
[3] J. Kärger, Phys. Rev. A **45**, 4173 (1992).
[4] K. Hahn and J. Karger, J. Phys. Chem. B **102**, 5766 (1998).
[5] C. Aslangul, *Proceedings of the 11th Max Born Symposium* (Springer-Verlag, Berlin, 1999), p. 326.
[6] L. Lizana and T. Ambjörnsson, Phys. Rev. Lett. **100**, 200601 (2008).
[7] L. Lizana and T. Ambjörnsson, Phys. Rev. E **80**, 051103 (2009).
[8] R. Besseling, R. Niggebrugge, and P. H. Kes, Phys. Rev. Lett. **82**, 3144 (1999); N. Kokubo, R. Besseling, and P. H. Kes, Phys. Rev. B **69**, 064504 (2004).
[9] S. Seidelin, J. Chiaverini, R. Reichle, J. J. Bollinger, D. Liebfreid, J. Britton, J. H. Wesenberg, R. B. Blackestad, R. J. Epstein, D. B. Hume, W. N. Itano, J. D. Joost, C. Langer, R. Ozeri, N. Shiga, and D. J. Wineland, Phys. Rev. Lett. **96**, 253003 (2006).
[10] B. Lin, M. Meron, B. Cui, S. A. Rice, and H. Diamant, Phys. Rev. Lett. **94**, 216001 (2005).
[11] V. D. Borman, B. Johansson, N. V. Skorodumova, I. V. Tronin,

V. N. Tronin, and V. I. Troyan, Phy. Lett. A **359**, 504 (2006).
[12] K. Nelissen, V. R. Misko, and F. M. Peeters, EPL **80**, 56004 (2007).
[13] M. Kollmann, Phys. Rev. Lett. **90**, 180602 (2003).
[14] S. Herrera-Velarde and R. Castaneda-Priego, J. Phys.: Condens. Matter **19**, 226215 (2007).
[15] G. Coupier, M. Saint Jean, and C. Guthmann, Phys. Rev. E **73**, 031112 (2006).
[16] G. Coupier, M. Saint Jean, and C. Guthmann, EPL **77**, 60001 (2007).
[17] C. Coste, J. B. Delfau, C. Even, and M. Saint Jean, Phys. Rev. E **81**, 051201 (2010).
[18] R. J. Ellis and A. P. Milton, Nature (London) **425**, 27 (2003).
[19] K. Hahn, J. Karger, and V. Kukla, Phys. Rev. Lett. **76**, 2762 (1996).
[20] J. Karger and D. M. Ruthven, *Diffusion in Zeolites and Others Microporous Solids* (Wiley Interscience, New York, 1992).
[21] Liying Wang, X. Gao, Z. Sun, and J. Feng, J. Chem. Phys. **130**, 184709 (2009).
[22] M. A. Lomholt, T. Ambjörnsson, and R. Metzler, Phys. Rev. Lett. **95**, 260603 (2005).
[23] A. D. Stroock, M. Weck, D. T. Chiu, W. T. S. Huck, P. J. A. Kenis, R. F. Ismagilov, and G. M. Whitesides, Phys. Rev. Lett. **84**, 3314 (2000).
[24] C. Dekker, Nat. Nanotechnol. **2**, 209 (2007).
[25] S. S. Nivarthi, A. V. McCormick, and H. T. Davis, Chem. Phys. Lett. **229**, 297 (1994).
[26] H. Jobic, K. Hahn, J. Kärger, M. Bee, A. Tuel, M. Noack, I. Girnus, and G. J. Kearley, J. Phys. Chem. B **101**, 5834 (1997).
[27] Q. H. Wei, C. Bechinger, and P. Leiderer, Science **287**, 625 (2000).
[28] B. Lin, B. Cui, J. H. Lee, and J. Yu, EPL **57**, 724 (2002).
[29] C. Lutz, M. Kollmann, P. Leiderer, and C. Bechinger, J. Phys.: Condens. Matter **16**, S4075 (2004).
[30] P. Galatola, G. Coupier, M. Saint Jean, J.-B. Fournier, and C. Guthmann, Eur. Phys. J. B **50**, 549 (2006).
[31] G. Coupier, C. Guthmann, Y. Noat, and M. Saint Jean, Phys. Rev. E **71**, 046105 (2005).
[32] M. Saint Jean, M. C. Even, and C. Guthmann, EPL **55**, 45 (2001).
[33] C. Rödenbeck, J. Kärger, and K. Hahn, Phys. Rev. E **57**, 4382 (1998).
[34] M. Berkowitz and J. A. McCammon, J. Chem. Phys. **75**, 957 (1981).
[35] J. R. Clem, Phys. Rep. **75**, 1 (1981).
[36] E. Durand, *Electrostatique* (Masson, Paris, 1966) (in French).